Mon. Not. R. Astron. Soc. **355,** 336–344 (2004) doi:10.1111/j.1365-2966.2004.07851.x

Gravitational waves from hyper-accretion on to nascent black holes

Rafael A. Araya-Góchez★

Theoretical Astrophysics, MC 130-33, California Institute of Technology, Pasadena, CA 91125, USA

Accepted 2004 March 17. Received 2004 February 18; in original form 2003 December 1

ABSTRACT

We examine the possibility that hyper-accretion on to newly born black holes occurs in highly intermittent, non-asymmetric fashion favourable to gravitational-wave emission in a neutrino-cooled disc. This picture of near-hole accretion is motivated by magnetorotationally induced, ultrarelativistic disc dynamics in the region of the flow bounded from below by the marginally bound geodesic radius $r_{\rm mb}$. For high spin values, a largely coherent magnetic field in this region has the dynamical implication of compact mass segregation at the displacement nodes of the non-axisymmetric, magnetorotational instability modes. When neutrino stress competes favourably for the disc dynamical structure, the matter clumps may be rather dense and sufficiently long-lived to excite the quasi-normal ringing (QNR) modes of the Kerr geometry upon infall. We find that this accretion flow may drive bar-like, quadrupole ($l, m = 2, 2$) modes in nearly resonant fashion for spin parameters $a \geqslant 0.9$. The ensuing build-up in strain amplitude of the undamped oscillations warrants a brisk rate of energy deposition into gravitational waves. A detectability assessment for the LIGO interferometers through the match filtering technique is given by integrating the energy flux over a one-second epoch of resonant hyper-accretion at 1 $\mathrm{M}_\odot\ \mathrm{s}^{-1}$. Thus, a 15-$\mathrm{M}_\odot$ Kerr black hole spinning at $a \simeq 0.98$ ($f_{\rm QNR} \simeq 1677$ Hz), and located at 27 Mpc (e.g. GRB 980425), will deliver a characteristic strain amplitude, $h_{\rm char} \simeq 2.2_{-21}$, large enough to be detectable by LIGO II. If resonant hyper-accretion were sustainable for a longer period (or at higher rates) possibly associated with a second broad hump in a gamma-ray burst light curve, these objects could be detected by LIGO I at very low redshifts.

Key words: black hole physics – gravitational waves – instabilities – MHD.

1 INTRODUCTION

It seems only fitting for ultrarelativistic, black hole accretion to be the leading contender to energize and explode the massive stars associated with gamma-ray bursts (GRBs) and hyper-novae. One must recognize, however, that such a scenario resides on a very exotic front: stellar-mass black holes accreting at 12 orders of magnitude above the Eddington limit! On the other hand, since GRB engines are effectively hidden from view, models of gravitational-wave emission may constitute the most effective probes into such enigmatic events. Indeed, today there is great impetus to address such an extreme accretion scenario and its associated, non-standard energy deposition channels. In this paper we are chiefly concerned with the possibility that the dynamical structure of hyper-accreting flows is highly intermittent on large scales, with the infall of large mass overdensities leading to prolific gravitational-wave emission coincident with the gamma-ray stage.

We envisioned the accretion-disc setting following the hyper-accreting black hole models of Popham, Woosley & Fryer (1999, hereafter PWF). For a fiducial scenario, $M_{\rm h} = 3\,\mathrm{M}_\odot$, $\alpha_{\rm SS} = 0.1$, and $\dot{M} = 0.1\,\mathrm{M}_\odot\ \mathrm{s}^{-1}$, these authors found that the onset of photodisintegration and of neutrino cooling at radii $r \lesssim 70\ [GM/c^2]$ yield a mildly advective, semithin, $\mathcal{H}_\Theta/r \lesssim 0.4$, accretion disc structure with a slightly sub-Keplerian rotation profile. An improved account of neutrino transport (Di Matteo, Perna & Narayan 2002) has found that the innermost disc portion should become optically thick to neutrinos for accretion rates $\dot{M} \gtrsim 0.1\,\mathrm{M}_\odot\ \mathrm{s}^{-1}$. This being the case, cooling by radial advection of energy will compete with that from local neutrino emission and advection will overwhelm neutrino cooling for $\dot{M} \gtrsim 1\,\mathrm{M}_\odot\ \mathrm{s}^{-1}$ (Di Matteo et al. 2002). Yet, such a high accretion rate is rather unlikely (MacFadyen et al. 2001), so we restrict our analysis to $\dot{M} \leqslant 1\,\mathrm{M}_\odot\ \mathrm{s}^{-1}$.

The structure of this paper is as follows. In Section 2, we assess the relevance of physical processes occurring in the relativistic region of the flow: $r_{\rm mb} \leqslant r \leqslant r_{\rm ms}$. Magnetorotationally induced, relativistic disc dynamics is addressed in Section 3, where we also discuss the role of compressibility and estimate the size of mass overdensities from a neutrino-cooled disc. In Section 4 we build an idealized, analytical model for gravitational-wave emission and, in Section 5, estimate the detectability of the gravitational wave (GW) signal for the LIGO interferometers with the match filtering technique.

★E-mail: arayag@tapir.caltech.edu

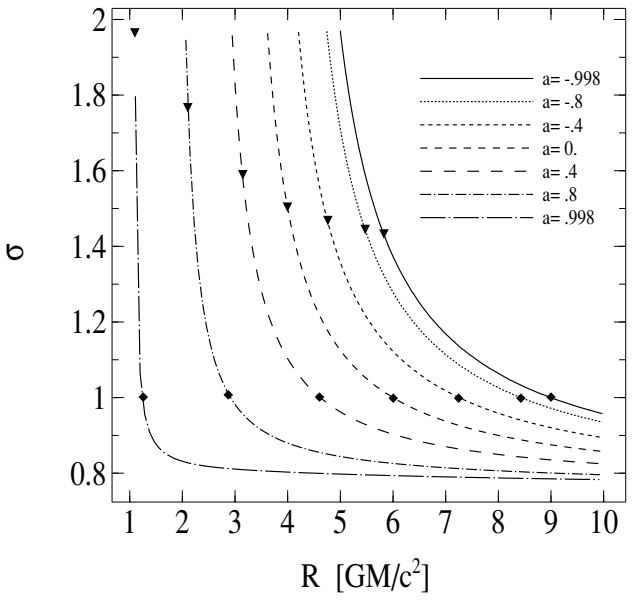

Figure 1. Normalized growth rate, $\hat{\sigma}$, as a function of radius for several values of the spin parameter a (from Araya-Góchez 2002).

2 PHYSICS INSIDE THE MARGINALLY STABLE RADIUS

The proposed model for gravitational-wave emission is based on the premise that large-scale magnetorotational effects will drive the disc dynamics in the ultrarelativistic region of the flow bounded from below by the marginally bound orbit radius. $r_{\rm mb}$ represents the lowest bound on the location of the cusp in the effective potential and is akin to a relativistic generalization of the inner Lagrangian point, L_1, for mass transfer in close binaries (Kozlowski, Jaroszyński & Abramowicz 1978). On the other hand, for spin rates $a \geqslant 0.9$, the growth rate of the magnetorotational instability (MRI), $\sigma_{\rm MRI}$, is faster than the inverse dynamical time-scale, Ω_+^{-1}, throughout the annulus $r_{\rm mb} \leqslant r \leqslant r_{\rm ms}$ by a factor $\simeq \mathcal{O}(2)$ (see Fig. 1). Thus, a small delay in reaching the 'free-fall' stage is all that is needed for magnetorotational dynamics to take place.

The exact location of the cusp depends on the source of free energy for the flow. Standard lore holds that the flow draws energy from the radial gradient in angular momentum and that since dissipation of angular momentum vanishes at $r_{\rm ms}$ for a Keplerian disc, this is where the inner edge of such a disc should reside (Novikov & Thorne 1973). Yet, we now know that when the disc dynamics is driven by magnetorotational effects the source of free energy is not the gradient in the radial distribution of angular momentum but rather the gradient in angular velocity;[1] that is, the source of free energy is the shear of the congruence of circular geodesics. Thus, MRI-mediated, turbulent angular momentum transport goes on unabated at the radius of marginal stability for cold geodesic orbits (Araya-Góchez 2002) and the flow within need not preserve specific angular momentum nor lose its relativistic Keplerian rotation profile in spite of the non-trivial radial velocity. We will therefore assume a Keplerian angular velocity profile throughout: $r \geqslant r_{\rm mb}$. This assumption is consistent with the models of PWF and Popham et al. (1999) – indeed, strong deviations from Keplerian rotation only occur as fluid elements approach the photon radius $r_{\rm ph}$ – and it is also consistent with global 3D simulations of non-radiative magnetohydrodynamic (MHD) accretion on to non-spinning black holes (Hawley & Krolik 2001; Hawley & Balbus 2002) in spite of partial pressure support for hot inner tori.

Inside $r_{\rm ms}$, the flow may not have time to cool significantly and advection of entropy will become progressively more important as the horizon, r_+, is approached. Entirely advective, accretion flows (i.e. non-radiative, hydrodynamical flows) are reckoned to possess a large, positive Bernoulli function $\mathcal{B} = \varrho + \int_0^p {\rm d}p\, \rho/\varrho$ (Abramowicz, Jaroszynski & Sikora 1978; Blandford & Begelman 2004) which makes the ultimate fate of accreting fluid particles a theme of controversy; e.g. ADAF (Narayan & Yi 1995a,b) versus CDAF (Narayan, Igumenshchev & Abramowicz 2000) versus ADIOS (Blandford & Begelman 1999, 2003). The broad conclusion drawn from this ongoing debate is that fluids with large internal energies, e.g. strongly magnetized fluids, are not easily accreted on to gravitational wells. In the ultrarelativistic flows of interest to us, and for large spin parameter a, the value of the relativistic enthalpy, $\varrho \equiv (\rho + \varepsilon + p)$, can be non-trivial $\varrho/\rho \geqslant 2$ (with magnetic energy folded into the internal energy ε), implying a high likelihood for a large Bernoulli function as well. We adopt the view that for a fluid with such high enthalpy, the dynamical boundaries set by the circular orbits of *cold* (point) particles in the Kerr geometry are inadequate.

3 MAGNETOROTATIONALLY INDUCED RELATIVISTIC DISC DYNAMICS

The MRI enables astrophysical mass accretion by promoting vigorous, turbulent transport of angular momentum. It also constitutes the key process to tap the free energy available in a flow endowed with differential rotation. Although linear mode analyses are based on the simplifying assumption of an initial laminar state, such analyses constitute a reasonable starting point to address the dynamical structure of the flow analytically. If the energy input at the outer scale of the turbulent cascade of the disc is the linear MRI (as suggested by the Lyapunov exponents derived in the shearing box simulations of Winters, Balbus & Hawley 2003), then the linear physics of the MRI is commensurate of the non-linear dynamical behaviour in what constitutes essentially a chaotic system. The analytical approach thus complements the outcome of present numerical experiments when appropriate. Indeed, the underlying physical regime is somewhat out of the reach of today' simulations although existing numerical work does provide a piecemeal physical understanding of the processes involved.

In the Newtonian picture, the MRI is essentially a local, comoving instability: the interplay of inertial accelerations with the elastic coupling of fluid elements creates an unstable state to the redistribution of specific angular momentum, $\ell(r)$, if the angular *velocity* profile decreases monotonically with radius. This criterion is in opposition to the (non-magnetic) Rayleigh criterion for stability of a differentially rotating fluid: $r^{-3}\, {\rm d}_r \ell^2 = \chi^2 \geqslant 0$, where χ is the frequency of radial epicyclic motions. Indeed, without the elastic coupling provided by the bending of field lines, such inertial forces – namely the shear (tide) and the Coriolis terms – induce stable radial epicyclic motions while preserving specific angular momentum.

Incompressible, MRI-initiated turbulence has a characteristic 'parallel' scale for fastest-growing modes corresponding to $k_\parallel \equiv \boldsymbol{k} \cdot \boldsymbol{1}_{\boldsymbol{B}} \simeq \Omega/v_{\rm Alf}$, and a normalized growth rate $\sigma = \hat{\rm A} \equiv 1/2\, {\rm d}_{\ln r} \ln \Omega$, associated with the shear parameter (also known as the Oort A 'constant'). The non-relativistic scale associated with the MRI is thus generally smaller than the vertical scaleheight of the disc by a factor $\mathcal{O}(v_{\rm Alf}/c_{\mathcal{H}})$. The geometrical bound on $k_\parallel$ when the field is vertical

[1] More generally, Balbus (2002) has found that for a magnetorotationally driven disc, the proper replacement of the classical Høiland stability criteria for rotational and convective motions involves the gradients in angular velocity and temperature instead of angular momentum and entropy.

corresponds to a half-wavelength fitting on the vertical scaleheight of the disc. For a toroidal field, the lowest bound on $k_\parallel$ is $1/r$ which would correspond to a supra-thermal field in the Newtonian picture (see, e.g. Foglizzo & Tagger 1995). Because of the possibility of large-scale, global disc dynamics, the latter modes are the focus of our analysis below.

3.1 Compressible non-asymmetric MRI modes

In the 2D regime of fastest growth, $k_\theta \gg k_r, k_\varphi$, non-axisymmetric, 'horizontal' displacement modes of a toroidal field have the following dispersion relation (Araya-Góchez 2002)

$$\hat{\sigma}^4 - \left[(\Lambda+1)\hat{q}^2_{\hat{\boldsymbol{B}}} + \hat{\chi}^2\right]\hat{\sigma}^2 + \Lambda\,\hat{q}^2_{\hat{\boldsymbol{B}}}\left(\hat{q}^2_{\hat{\boldsymbol{B}}} + 4\hat{\mathrm{A}}\right) = \emptyset, \tag{1}$$

where all frequencies are normalized to the rotation rate, $\hat{\mathrm{A}} \equiv 1/2\,\mathrm{d}_{\ln r}\ln\Omega$ is the Oort A 'constant', $\hat{\chi}^2 \equiv 4(1+\hat{\mathrm{A}})$ is the square of the epicyclic frequency, and $\hat{q}_{\hat{\boldsymbol{B}}} \equiv (\boldsymbol{k}\cdot\boldsymbol{v}_{\mathrm{Alf}})/\Omega$ is a frequency related to the component of the wavevector along the field (in velocity units).

Λ is defined through

$$\Lambda \equiv \frac{\Gamma}{\Gamma+\Theta} \tag{2}$$

where Γ is the adiabatic index and $\Theta \equiv p_{\boldsymbol{B}_\varphi}/p_{\mathrm{r+g}}$. This definition entrains an important anisotropy constraint on the Lagrangian displacement vector field $\boldsymbol{\xi}$ (Foglizzo & Tagger 1995): $v^2_{\mathrm{Alf}}(\boldsymbol{k}_\perp\cdot\boldsymbol{\xi}_\perp) = -c_s^2(\boldsymbol{k}\cdot\boldsymbol{\xi})$, as well as the compressibility characteristics of non-axisymmetric modes

$$\frac{\Delta\rho}{\rho} = (1-\Lambda)(-\mathrm{i}k_\parallel\xi_\parallel) \tag{3}$$

where Δ denotes the Lagrangian perturbation (recall the non-relativistic relation between Lagrangian and Eulerian perturbations $\tilde{\Delta} = \delta + \boldsymbol{\xi}\cdot\nabla$). The compressibility of the modes is an imprint on the deviations of Λ from unity. A word of caution here regards the peculiar behaviour of the fluid when the internal stress has heat-conduction characteristics, e.g. photon or neutrino pressure (see Section 3.3). From equation (3), one sees that the degree of compression of the modes gets stronger with the field strength and, naturally, with a softer equation of state. Note that setting $\Lambda \doteq 1$ in the dispersion relation (1) yields the incompressible, local variant of the MRI.

From equation (1), the parallel wavenumbers of fastest growth satisfy (see also Foglizzo 1995)

$$\hat{q}^2_{\hat{\boldsymbol{B}}} = -2\hat{\mathrm{A}} + \left(\frac{1+\Lambda}{2\Lambda}\right)\times\left\{-\frac{2\Lambda\hat{\mathrm{A}}^2}{D}\right\} \overset{\Lambda\to 1}{\longrightarrow} -\hat{\mathrm{A}}(2+\hat{\mathrm{A}}),$$
$$\text{where } D \equiv 1 + \left(\frac{1-\Lambda}{2}\right)\hat{\mathrm{A}} + \sqrt{1+(1-\Lambda)\hat{\mathrm{A}}}, \tag{4}$$

while the expression in the curly brackets corresponds to the square of the growth rate for compressible modes.

3.2 General relativistic effects in the Cowling limit

General relativity modifies the Newtonian results in that it introduces large-scale effects when shear begins to overwhelm the Coriolis terms, i.e. as r_{ph} is approached (see equations 32 of Araya-Góchez 2002). Although the hole is likely to be born in an excited state, e.g. away from its asymptotic, Kerr geometry, we work in the Cowling limit, $\delta g \doteq \emptyset$, and, to zeroth order, use the standard form of the Kerr metric in the equatorial plane (Boyer–Lindquist coordinates):

$$\mathrm{d}s^2 = -\frac{\mathcal{D}}{\mathcal{A}}\mathrm{d}t^2 + r^2\mathcal{A}(\mathrm{d}\varphi - \omega\,\mathrm{d}t)^2 + \frac{1}{\mathcal{D}}\,\mathrm{d}r^2, \tag{5}$$

with $\omega \equiv 2a/\mathcal{A}r^3$ the rate of frame dragging by the hole and where the metric functions of the radial BLF coordinate are written as relativistic corrections (e.g. Novikov & Thorne 1973):

$$\mathcal{A} \equiv 1 + \frac{a^2}{r^2} + 2\frac{a^2}{r^3}, \text{ and } \mathcal{D} \equiv 1 - \frac{2}{r} + \frac{a^2}{r^2},$$

in normalized geometrical units ($c = G = M_{\mathrm{bh}} = 1$).

For circular, incompressible, geodesic flow, the dispersion relation near a rotating hole is given by (Araya-Góchez 2002)

$$(\gamma\sigma)^4 - \left[2q^2_{\hat{\boldsymbol{B}}} + 4\gamma^2\Omega^2_\pm\left(\mathcal{C}_\pm - \frac{3}{4}\mathcal{D}\right)\right](\gamma\sigma)^2 + q^2_{\hat{\boldsymbol{B}}}\left[q^2_{\hat{\boldsymbol{B}}} - 4\left(\frac{3}{4}\gamma^2\mathcal{D}\,\Omega^2_\pm\right)\right] = \emptyset \tag{6}$$

where γ is the redshift factor, $\mathcal{D} = g_{rr}^{-1}$, and

$$\mathcal{C}_\pm \equiv 1 - \frac{3}{r} \pm \frac{2a}{r^{3/2}}$$

corresponds to the $\mathcal{C}$ function of Novikov & Thorne (1973) for prograde (+) orbits. With regard to the electromagnetic stress, the only difference from the non-relativistic, incompressible analogue is that the Alfvén speed is now weighted by the relativistic enthalpy of the fluid (Araya-Góchez 2002)

$$\varrho v^2_{\mathrm{Alf}} \equiv \frac{1}{2}F^{\mu\nu}F_{\mu\nu}. \tag{7}$$

Factoring out the orbital frequency $u^\varphi/u^t \equiv \Omega_\pm = \pm(r^{3/2}\pm a)^{-1}$ and with $\gamma\sigma \equiv \Omega_\pm\,\hat{\sigma}$, one has

$$\hat{\sigma}^4 - \left(2\hat{q}^2_{\hat{\boldsymbol{B}}} + \hat{\chi}^2_\pm\right)\hat{\sigma}^2 + \hat{q}^2_{\hat{\boldsymbol{B}}}\left(\hat{q}^2_{\hat{\boldsymbol{B}}} + 4\hat{\mathrm{A}}\right) = \emptyset \tag{8}$$

where

$$\hat{\mathrm{A}} \equiv -\frac{3}{4}\gamma^2\mathcal{D} \text{ and } \hat{\chi}^2_\pm = 4\gamma^2\left(\mathcal{C}_\pm - \frac{3}{4}\mathcal{D}\right)$$

denote the normalized shear parameter and comoving epicycle frequency ($\gamma^{-1}\,\hat{\chi}$ corresponds to the epicycle frequency as measured at asymptotic infinity). Thus, with the proper generalizations of the epicycle frequency and shear parameter, the local dispersion relation is identical with the Newtonian case in the limit of no fluid compression, cf. equations (1) and (3) with $\Lambda \to 1$.

Next, using the relation $\gamma^2 = (1 \pm a/r^{3/2})^2\,\mathcal{C}_\pm^{-1}$ for circular, cold, geodesic flow (Novikov & Thorne 1973), one finds the fastest-growing modes will conform with

$$\hat{q}^2_{\hat{\boldsymbol{B}}} = 1 - \frac{1}{16}\hat{\chi}^4 = 1 - \left(1 \pm \frac{a}{r^{3/2}}\right)^4\left(1 - \frac{3}{4}\,\frac{\mathcal{D}}{\mathcal{C}_\pm}\right)^2 \tag{9}$$

which remains finite and close to the Newtonian value $\hat{q}_{\hat{\boldsymbol{B}}} \to -\hat{\mathrm{A}}(2+\hat{\mathrm{A}}) = 15/16$ for all radii outside of the ISCO.

Recall that the marginally stable orbit (also known as the ISCO), r_{ms}, corresponds to the root of $\hat{\chi}_\pm = 0$. The radius of the circular photon orbit, r_{ph}, is where $\mathcal{C}_\pm = 0$ and the event horizon, r_+, happens at the outer root of $\mathcal{D} = 0$. For any value of the rotation parameter a: $r_{\mathrm{ms}} > r_{\mathrm{mb}} > r_{\mathrm{ph}} > r_+$. Our statement on large-scale effects follows from these remarks and from direct inspection of equation (9): $\hat{q}_{\hat{\boldsymbol{B}}} \to 0^+$ as $r \to r^+_{\mathrm{ph}}$, i.e. the most unstable MRI modes go to large scales as the photon orbit is approached. Figs 1 and 2 show the general trends for the normalized growth rate and wavenumbers as functions of radius and spin parameter.

Two notable oversimplifications of this relativistic approach involve the global disc structure and the compressibility of the modes.

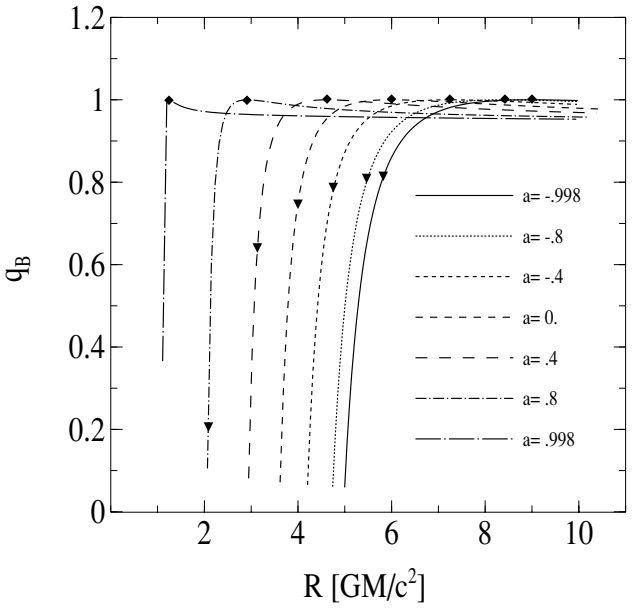

Figure 2. Normalized parallel wavenumber, $\hat{q}_{\hat{\boldsymbol{B}}}$, as a function of radius (in gravitational radii) for several values of the spin parameter a. Diamonds indicate the location of the marginally stable orbit, $\hat{\chi} \doteq \emptyset$, and triangles denote the location of the marginally bound orbit (from Araya-Góchez 2002).

We discuss these in turn. Curvature effects and radial field structure will indeed modify the dispersion relation [2] (see, e.g. Curry & Pudritz 1995; Ogilvie & Pringle 1996) but these effects are unlikely to modify the gross properties of the fastest-growing modes unless radial stratification plays a destabilizing role. Furthermore, we note here and *correct* our previous comment (Araya-Góchez 2002): a large coherence length-scale for the field, *does not* necessarily imply a dynamical transition from a centrifugally driven to magnetically driven disc. $\hat{q}_{\hat{\boldsymbol{B}}} \to 0^+$ is merely a statement about the length-scale of the fastest-growing modes, $k_\parallel^{-1} \simeq \mathcal{O}(\tilde{r})$, regardless of field strength. On the other hand, the compressibility of the modes alters the threshold of shear parameter where $\hat{q}_{\hat{\boldsymbol{B}}} \to 0^+$, but does not fundamentally affect the conclusions drawn from equation (9) either. For roughly equal neutrino and radiation pressures (see below), one can use an effective adiabatic index (Araya-Góchez & Vishniac 2004) in equation (4) to anticipate that the effects of compressibility on toroidal modes is to increment the threshold of the shear parameter where $\hat{q}_{\hat{\boldsymbol{B}}} \to 0^+$ from $-\hat{\mathrm{A}} = 2$ to $-\hat{\mathrm{A}} \to 1 + 2D/(1+\Lambda)$; cf. equation (4). Nevertheless, since for geodesic flow $\hat{\mathrm{A}} \propto \mathcal{D}/\mathcal{C}_\pm$ and $\mathcal{C}_\pm \to 0$ as $r \to r_{\rm ph}$, the increase in shear threshold in this setting is rather inconsequential.

3.3 Heat conduction and clump scale

A precise assessment of radiative diffusion effects in the general relativistic regime is hampered by the breakdown of a key assumption made to simplify the 'linear poking' of the Faraday field tensor (Araya-Góchez 2002): use of the enthalpy-weighted specific four magnetic field in equation (7). However, just as in radiation-pressure-dominated fluids, one expects a neutrino-stress-dominated gas – with neutrinos semicontained by the nucleon component through scattering – to comprise a rather peculiar MHD fluid. When a fluid transitions into a radiative pressure regime, compressive modes will lose pressure support in a given range of wavenumbers (Agol & Krolik 1998). Thus, the magnetic field is truly frozen only to the comoving volume associated with the baryon component and compressive perturbations need not behave adiabatically.

The optical half-depth to scattering of a standard radiation-pressure-dominated α-disc (Shakura & Sunyaev 1973)is related to the scaleheight, $\mathcal{H}$, and rotation rate, Ω, by $\tau_{\rm disc} = -c/(2\alpha\hat{\mathrm{A}}\Omega\mathcal{H})$. This relation is explicitly sensitive only to the local nature of the cooling but is implicitly subject to a suitable vertical gradient of heat deposition (see, e.g. Krolik 1999). Therefore, these scalings also hold for a neutrino-cooled α-disc through a replacement in the source of opacity by neutrino scattering in the non-advective accretion regime: $0.1\,\mathrm{M}_\odot\,\mathrm{s}^{-1} \leqslant \dot{M} \leqslant 1\,\mathrm{M}_\odot\,\mathrm{s}^{-1}$. On the other hand, in the Newtonian regime, $\hat{q}_{\hat{\boldsymbol{B}}} \simeq \mathcal{O}(1)$, and for magnetic angular momentum transport such that $\alpha \simeq v_{\rm Alf}^2/c_{\mathcal{H}}^2$, the depth through the MRI eddies is $\tau_{\rm eddy} \sim v_{\rm Alf}/c_{\mathcal{H}} \times \tau_{\rm disc} \sim c/(2\hat{\mathrm{A}}\sqrt{\alpha}c_{\mathcal{H}}) \gg 1$. Thus, assuming an isotropic random walk for neutrinos, the diffusion time through these eddies, $t_{\rm diff} \sim \Omega^{-1}$, is similar to the time-scale for fastest MRI modes to develop, $t_{\rm MRI} \simeq -\mathrm{A}_{\rm Oort}^{-1}$.

Radiative heat conduction will isotropize the dynamically dominant modes since neutrinos will diffuse through the smallest distance associated with the eddies, i.e. mostly in the vertical direction. In our problem, this will diminish the growth rate of the instability (Blaes & Socrates 2001) but not by much. If neutrino stress were predominant, the horizontal regime of fastest growth (e.g. Section 3.1) would be inaccessible; yet, this is never the case in neutrino-cooled discs since the pressure contributions from radiation and pairs (non-diffusive components) and neutrinos (diffusive component) all have the same temperature dependence, $a/6T^4$, with the relative contributions varying only by internal degrees of freedom times particle statistics factors (with only one helicity state for neutrino pairs): $2 \times 1, 4 \times 7/8$, and $6 \times 7/8$, respectively. Thus, p_ν is never greater than about $\simeq p_{\rm rad}$ where $p_{\rm rad} = 11/12aT^4$ includes the pressure from pairs and photons.

Let us quantify these arguments in order to gauge the length-scale of the clumps. At a very fundamental level, clump formation is intimately connected to the effects of radiative heat conduction out of compressive perturbations. This can be understood by writing down the polarization properties of the fastest-growing modes in the horizontal regime: $\xi_r = -\sqrt{\Lambda}\xi_\varphi$ and $|\xi_\theta| \ll |\xi_r|$, and reading from equation (3) that at the linear stage of the instability there exists a converging flow toward the Lagrangian displacement node of the modes (see fig. 2 of Foglizzo & Tagger 1995). In a fluid with entirely elastic (adiabatic) properties, the pressure perturbation associated with such compression will act as a restoring force to decompress the fluid in the non-linear stage. On the other hand, when the fluid has radiative heat conduction properties on the scale of the density perturbations, no such restoring force persists on time-scales longer than the inverse of the growth rate so the clumps will survive for longer times. Turner, Stone & Sano (2002) and Turner et al. (2003) report that in a standard radiation-pressure-dominated disc, when $p_{\rm rad} \gtrsim p_{\rm gas} \simeq p_{\boldsymbol{B}}$, the non-linear outcome of the MRI is a porous medium with drastic density contrasts. Under nearly constant total pressure and temperature, the non-linear regime shows that density enhancements anticorrelate with azimuthal field domains – just as expected from the linear theory – and that turbulent eddies live for about a dynamical time-scale while mass clumps are destroyed through collisions or by running through localized regions of shear on a similar time-scale. Notably, the non-linear density contrasts

[2] The interested reader is invited to compare the relativistic, local version of the equations of motion for ξ, equations (32) of Araya-Góchez (2002), with the Newtonian, global version equations (2.6) and (2.7) of Ogilvie & Pringle (1996).

may be quite large, $\langle \rho_{\rm max}/\rho_{\rm min}\rangle \gtrsim \mathcal{O}(10)$. We make no attempt here to estimate $\Delta\rho/\rho$ from the linear theory but rather argue that when the length-scale of the instability is suitable large, $\lambda_{\rm MRI} \simeq \mathcal{O}(\tilde{r})$ (see below), a fraction of $\mathcal{O}(1/2\pi)$ of the mass in the annulus $r_{\rm mb} \leqslant r \leqslant r_{\rm ms}$ will reside in one massive clump such that the gravitational-wave emission associated with the infall of this clump will dominate the power spectrum.

Let us emphasize that the isotropic size of the clumps is determined by the condition that, on the time-scale of the instability, neutrinos will diffuse through the clumps via nucleon scattering (Araya-Góchez & Vishniac 2004). For simplicity, we again assume local balance of dissipation from the shear flow with cooling from neutrino emission and a constant supersonic Mach number for the disc flow: $M_\varphi = v^{\bar{\varphi}}/c_{\mathcal{H}}$ ($M_\varphi = 2.5$ is consistent with the results of PWF in the neutrino-cooling regime). Under this assumption, we need not worry about detailed neutrino transport and, relaxing the condition $\hat{q}_{\hat{B}} \approx 1$, the size of the most massive clumps will correspond to

$$l_{\rm clump} \simeq v_{\rm Alf}/c_{\mathcal{H}}\mathcal{H} \sim \sqrt{\alpha} M_\varphi^{-1}\tilde{r}.$$

Thus, in the relativistic regime the length-scale of the clumps will be smaller than the scale associated with the fastest-growing modes by a factor of $\mathcal{O}(\hat{q}_{\hat{B}})$.

4 A SIMPLE PHYSICAL MODEL FOR GRAVITATIONAL-WAVE EMISSION

The key to our argument for clumpy, near-hole hyper-accretion is based on the observation that the length-scale of the fastest-growing modes may be quite large at the innermost disc boundary, $r_{\rm mb}$. Since the radial velocity is non-negligible, one cannot demand 'tightly fitting' eigenmodes on the circumference at fixed radius. Loosely speaking, the WKB modes live on ingoing spiral trajectories (see Section 4.2); but we are only concerned with their overall gross properties.

The clumps form very rapidly, $t_{\rm MRI}^{-1} \simeq \Omega\hat{\sigma}$, and very close to the horizon. Since these are very compact, $l/\tilde{r} \simeq \mathcal{O}(0.1)$, we considered them as point particles in the order of magnitude estimate of gravitational-wave emission below. Computation of accurate waveforms for the infall of a single clump constitutes a daunting task because of the non-trivial multipole contributions to the radiation field in the strong gravity regime near $r_{\rm mb}$. The contributions from higher than quadrupole will broaden the power spectrum of emitted waves (Zerilli 1970; Davis et al. 1971, hereafter DRPP) and recent results by Lousto & Price (1997, hereafter LP97) show that particles released from very near the marginally bound orbit of a non-spinning hole – or more precisely near the maximum of the Zerilli potential – will maximize the locally radiated energy.

As a 'back of the envelope' estimate of the quadrupole rms strain, $|h| = \sqrt{h_+^2 + h_\times^2}$, associated with the infall of a single clump, we simply assume that the clump is formed above $r_{\rm mb}$ and that it survives for one rotation period before plunging into the hole. The transverse-traceless projection of the metric perturbation in the radiation zone, $h_{ij}^{\rm TT}$, is estimated by replacing the second time derivative of the mass quadrupole moment, $\partial_t^2\mathcal{J}_{ij}^{\rm TT}$, by the kinetic energy associated with non-spherical motion; i.e. clump rotation as seen at asymptotic infinity (Thorne 1987). Thus

$$|h| = |h_{ij}^{\rm TT}| \equiv \frac{2}{d}\left(\frac{G}{c^4}\right)\left|\partial_t^2\mathcal{J}_{ij}^{\rm TT}(t-r)\right| \simeq \left(\frac{G}{c^4}\right)\frac{\tilde{r}^2\Omega^2}{d}\delta M \simeq \frac{G\delta M}{(c^2 d)}.$$

For a 15-$M_\odot$ black hole rotating at $a = 0.98$, and accreting $1\,M_\odot\ {\rm s}^{-1}$, the mass in the clumps is $\delta M \simeq \dot{M}/\Omega \simeq 1.8_{-4}\,M_\odot$, where $\Omega(r_{\rm mb}) \simeq 0.4 = 5400$ Hz, corresponding to a linear frequency $\Omega(r_{\rm mb})/\pi = 1720$ Hz. This gives $|h| \simeq 3.2_{-25}$ for a source at 27 Mpc. To bring this into the LIGO band, $|h|_{\rm eff} \simeq 1._{-21}$ one would need to integrate over $N \simeq 1_{+8}$ cycles or over 1700 s! Thus, the rms strain associated with infall of a single clump on to the hole is too small to be of any astrophysical importance at present.

But this issue is more subtle than it appears at first sight.

4.1 Quasi-normal ringing waveforms: single excitation event

Since the clumps form in a strong gravity regime, the process of gravitational-wave emission from infall at such a short range must be cast as an excitation of the infinite number of increasingly damped quasi-normal modes of oscillation of the background geometry (Leaver 1985). The often-drawn analogy for such quasi-normal ringing (QNR) of the hole to the ringing of a bell is fundamentally flawed in at least one respect: the black hole is not excited by the smashing of the clump as it 'hits' the horizon. Rather, the hole is excited when the metric perturbation associated with the clump is 'felt' by the background metric. The excitation event therefore constitutes a smooth process whereby infall of a clump from $\simeq r_{\rm mb}$ and through r_+ serves as a source in the Teukolsky (1973) equation for small perturbations of the Kerr geometry (with appropriate boundary conditions at r_+ and r_∞). This is an important distinction with a great deal of relevance to the problem at hand since we need to gauge the 'driving' of QNR modes in terms of an effective coupling from clump infall.

Clumpy black hole accretion from an exterior disc will excite preferentially quadrupole, bar-like mode perturbations of the geometry with spheroidal harmonic indices [3] $(l, m) = (2, 2)$. An approximate analytical expression for the QNR frequency of this mode is given by Echeverria (1989):

$$\omega_{22} = \left[1 - 0.63(1-a)^{3/10}\right] \times \left[1 + \frac{\rm i}{4}(1-a)^{9/20}\right]. \qquad (10)$$

The corresponding quality factor, also known as the Q-value, of the (2, 2) mode

$$Q_{22}(a) \equiv \frac{1}{2}\frac{\Re[\omega_{22}]}{\Im[\omega_{22}]} = 2(1-a)^{-9/20}, \qquad (11)$$

is $\geqslant 2\pi$ for $a_{\rm crit} \geqslant 0.92$ This represents a minimum value of a to regard the hole as a decent bar-like mode oscillator. Below $a_{\rm crit}$ the mode is damped too strongly to allow for any significant build-up of the strain signal/spectrum from resonant accretion (see below).

In the radiation zone and time domain, undriven QNR waveforms constitute circularly polarized, damped oscillations (Leaver 1985; Echeverria 1989)

$$h(t) \equiv h_+ - {\rm i}h_\times = \frac{H_0}{d}S_{22}(\phi, \theta, a){\rm e}^{-{\rm i}(\omega_{22}t - \varphi)} \qquad (12)$$

where d is the luminosity distance to the source, and $S_{22}(\phi, \theta, a)$ is a spin weighted, normalized ($\int {\rm d}\Omega |S_{22}|^2 = 1$), spheroidal harmonic of coordinates ϕ and θ [in the Schwarzschild limit $S_{22}(\phi, \theta, a \to 0) \longrightarrow Y_{22}(\phi, \theta)$]. The strain length amplitude of

[3] Quadrupole perturbations, $l = 2$, are reckoned to contribute about 90 per cent of the energy budget for outgoing GWs while $l = 4$ modes add about 10 per cent. Higher multipole contributions are negligible, see, e.g. DRPP, LP97.

the waveform, H_0 (in units of the hole mass M), and the phase shift, φ, depend on the initial conditions of the metric perturbation.

H_0 gauges the efficiency of the emission process to posit a fraction of the total rest-mass energy of the system into outgoing gravitational-wave energy. For strong excitation events such as binary black hole coalescence, this fraction may be as large as 3 per cent (see, e.g. Flanagan & Hughes 1998). For the infall of a clump of mass $\delta M \ll M$, this fraction scales as $\varepsilon\,(\delta M)^2/M$ (DRPP), with a corresponding time-domain strain amplitude $\propto \sqrt{\varepsilon}\,\delta M/\sqrt{M}$. The precise value of ε for a rotating hole is unknown, but it hovers on a few per cent for the perturbations of a Schwarzschild geometry induced by radial infall from infinity[4] (DRPP). For non-axisymmetric perturbations, the energy released from clump infall may be considerably larger (Fryer, Holz & Hughes 2002) and for nearly resonant, driven oscillations from hyper-accretion, we demonstrate below that the total amount of energy deposited into outgoing gravitational waves is only bounded from above by a factor of a few times the rest-mass energy of a single clump!

4.2 Collective effects: resonant driving of QNR modes

To assess the free-fall stage of the clumps, we recall from Section 2 that the cusp in the effective potential occurs somewhere above $r_{\rm mb}$ (depending on the angular velocity profile) and that a relativistically hot accretion flow may posses a semi-Keplerian angular velocity profile, $\Omega_+ = (r^{3/2} + a)^{-1}$, down to this region (PWF, Popham & Gammie 1998; Hawley & Krolik 2001). Parametrizing the accretion flow through its Mach number and the angular momentum transport through a Shakura–Sunyaev 'α' parameter (as in Section 3.3, we adopt $M_\varphi \doteq 2.5$ and $\alpha \doteq 0.1$), when $a \gtrsim 0.9$ the wavelength associated with the fastest-growing MRI modes becomes comparable with $2\pi\tilde{r}$ at a radius $r \geqslant r_{\rm mb}$; e.g. when $\hat{q}_{\hat{\boldsymbol{B}}} \simeq 0.126\sqrt{\alpha_{0.1}}\,{\rm M}_{\varphi,2.5}^{-1}$. At higher spin parameter values, MRI modes go to comparably large scales at radii closer to $r_{\rm ms}$. Thus, the annulus $r_{\rm ms} \geqslant r \geqslant r_{\rm mb}$ constitutes a relativistic locus for large-scale magnetorotationally induced fluid dynamics at moderately large values of black hole spin: $a \geqslant 0.9$.

Since the radial velocity is non-negligible, MRI wave modes must be interpreted as WKB modes that live on in-spiral trajectories. For the sake of simplicity in the discussion below, presume that fluid elements undergo one full rotation in the annulus $r_{\rm ms} \geqslant r \geqslant r_{\rm mb}$ before 'plunging in' from $r_{\rm mb}$. The integrated phase along this path can be interpreted with a skewed effective wavelength which goes to increasingly larger length-scales as fluid particles approach $r_{\rm mb}$. If we demand a tight fit of one whole, integrated WKB wavelength on the in-spiral trajectory between $r_{\rm ms}$ and $r_{\rm mb}$, the mid-Lagrangian displacement node, $\boldsymbol{\xi}(\tau) = 0$, represents a converging point for the flow in the linear stage of the instability as seen by a comoving geodesic observer. This node subsequently develops into the mass overdensity that we identify with a clump in the non-adiabatic stage (i.e. when neutrinos have diffused out of the compressive perturbation, Section 3.3). Since the scale of the mode is larger downstream of the displacement node, most of the mass in the overdensity will be advected in from fluid particles that rush upstream toward the node on the instability time-scale; a smaller fraction of the mass of the clump flows downstream toward the node, from smaller scales upstream.

When the effective WKB scale on the instability is suitably large, a reasonably large fraction of the mass in the annulus will reside in a single clump by the time it reaches $r_{\rm mb}$. The subsequent 'free-fall' from $r_{\rm mb}$ (presuming this radius corresponds to the cusp in effective potential; e.g. Abramowicz et al. 1978; Kozlowski et al. 1978), occurs on a dynamical time-scale $t_{\rm dyn} \equiv \Omega_+^{-1}(r_{\rm mb})$. Furthermore, since l-pole modes couple to the l-multipole of the dynamical frequency (e.g. Ex. 3.7 of Rybicky & Lightman 1979), the driving frequency for quadrupole oscillations corresponds to twice the relativistic Keplerian frequency at $r_{\rm mb}$: $\omega_{\rm dr} \equiv 2\Omega_+(r_{\rm mb})$. Remarkably, *the difference between the driving frequency and the resonant (2, 2) QNR frequency resides within a factor of the order of the damping rate throughout the range* $0.9 \lesssim a \lesssim 0.99$ (Fig. 3); whereas the Q-value of the mode hovers in $5.6 < {\rm Q} < 33$. This picture of hyper-accretion portrays an ideal scenario to drive the QNR modes of the hole resonantly, were the clumps to arrive at $r_{\rm mb}$ steadily, with a small spread around time intervals of $\mathcal{O}(\Omega_+^{-1})$, and for long enough to build the strain amplitude up to saturation point, or about 2Q cycles. Yet, nature will add randomness to the process.

The degree of stochasticity in the arrival times of the clumps is related to the temporal distribution of density perturbations in the outer flow (e.g. for $r > r_{\rm ms}$). This flow is turbulent on small scales, $\ell_{\rm turb} \ll r$, so the growth of heavier mass overdensities should occur by aggregation of smaller density fluctuations. Notwithstanding this fact, in the picture of clump formation outlined above, most of the mass in the clump is advected in from downstream of a displacement node where the WKB modes attain large scales. Thus, large-scale magnetorotational dynamics downstream of a forming clump will minimize the impact of small-scale density perturbations upstream if the flow is steady on the dynamical time-scale (simulations that include black hole spin – e.g. De Villiers, Hawley & Krolik 2003 and Hirose et al. 2004 – yield rms fluctuations in $\dot{M}$ of order 20 per cent near $r_{\rm ms}$). In this quasi-linear picture, the probability distributions

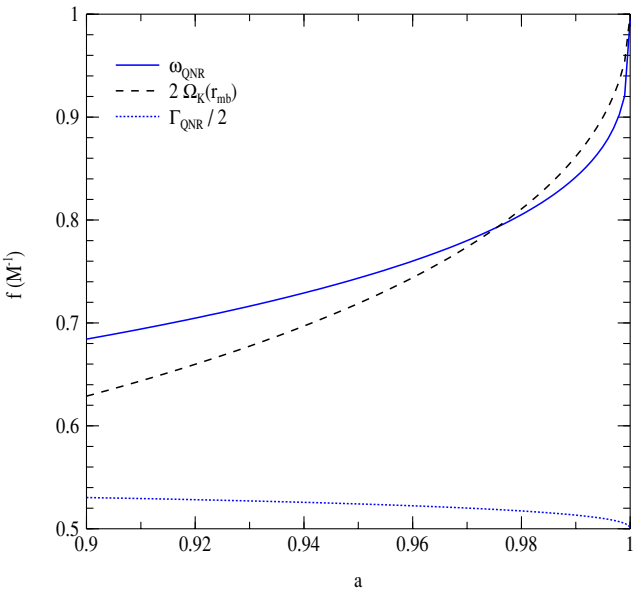

Figure 3. The real part of the QNR frequency, $\omega_{\rm QNR}$, and the driving frequency, $\omega_{\rm dr} = 2\,\Omega_+\,(r_{\rm mb})$, for quadrupole oscillations as functions of the spin parameter, a, of the hole. Plotted also is half of the imaginary part of the QNR frequency offset by $+0.5$ from zero for ease of comparison with the difference among the other two frequencies. Most notable is the fact that throughout the range $a \geqslant 0.95$, $|\omega_{\rm QNR} - \omega_{\rm dr}| \leqslant 1/2\Gamma_{\rm QNR}$, which implies resonant driving of the QNR modes from hyper-accretion.

[4] Strictly speaking, the energy released in this case includes not just the ringing phase but also a small contribution from the gravitational bremsstrahlung component, see, e.g. LP97.

for clump arrival time and clump mass would be correlated, with heavier clumps arriving semiregularly and superimposed on a more diffusive and stochastic component of the accretion flow. Since a detailed probability distribution of arrival times is beyond the scope of this study, below we simply assume that the probability distribution for arrival times will favour resonant driving of the modes with a moderate spread around the resonant frequency of arrival times (see further discussion on this point below). Lastly, note that the arguments above do not depend on in-spiral trajectories wrapping around fully on the annulus; since the MRI time-scale is suitable fast, a small delay to reach the free-fall stage is all that is needed for MRI dynamics to act.

Beyond an initial transient period where the amplitude of the oscillation builds up to saturation point, driven QNR oscillations become *undamped* oscillations at the driving frequency

$$h(t) = \frac{H_0}{d}\frac{\omega_{\rm QNR}^2}{\omega_{\rm dr}^2-\omega_{\rm QNR}^2-{\rm i}\,\omega_{\rm dr}\Gamma_{\rm QNR}}S_2^2(\phi,\theta,a)\,{\rm e}^{-{\rm i}\,\omega_{\rm dr}t} \equiv \frac{H_{\rm sat}}{d}S_{22}(\phi,\theta,a){\rm e}^{-{\rm i}\,(\omega_{\rm dr}t+\delta_t)}, \quad (13)$$

where $\delta_t = \tan^{-1}[\omega_{\rm dr}\Gamma_{\rm QNR}/\,(\omega_{\rm dr}^2-\omega_{\rm QNR}^2)]$ is a slowly varying function of time and the saturation amplitude, $H_{\rm sat}$, represents an effective strain length (in units of the total mass, M, of the system) set by the condition that the energy input from clump infall ($\propto H_{\rm sat}$) be balanced by the damping losses ($\propto H_{\rm sat}^2$). When the driving frequency is near resonance, $H_{\rm sat}$ is limited primarily by the natural[5] damping of the QNR mode, $\Gamma_{\rm QNR}\equiv\Im\,[\omega_{22}]$, and secondarily by the relative difference of the driving frequency to the resonant frequency for quadrupole ringing, $\omega_{\rm QNR}\equiv\Re\,[\omega_{22}]$. Furthermore, since $\omega_{\rm dr}\approx\omega_{\rm QNR}$ for a relatively broad range of a values (Fig. 3), the resonant frequency may be taken to be $\omega_{\rm QNR}$.

The energy flux carried away by driven QNR waveforms benefits greatly from the build-up in the amplitude of the strain, $H_{\rm sat}$, when compared to the ringing from a single excitation event H_0 (cf. equation 12). Indeed, when driven near resonance the augmented amplitude is proportional to twice the Q-value of the mode: $H_{\rm sat}|_{\omega_{\rm dr}=\omega_{\rm QNR}} = 2\,{\rm Q}\,H_0$ (cf. equation 11). Although the modes are driven precisely at resonance only for $a\approx 0.98$, note from Fig. 3 that $|\omega_{\rm QNR}-\omega_{\rm dr}|\leqslant\Gamma_{\rm QNR}$ throughout the range $0.90\lesssim a\lesssim 0.99$. This sets a lower bound on the augmented strain amplitude for this range of a: $H_{\rm sat}/H_0\gtrsim{\rm Q}$ (recall that the resonant denominator only looks like a Lorentzian very near the resonance). Fig. 4 shows the exact value of the augmented strain amplitude for $a\geqslant 0.9$. Furthermore, adopting a very modest $\varepsilon_0 = 0.02$ for the infall of a single clump (in accordance with the DRPP and LP97 results; see also discussion in Section 4.1), the augmented efficiency factor in GW energy deposition from driven oscillations $\varepsilon = (H_{\rm sat}/H_0)^2\,\varepsilon_0$ may be larger than unity. Depending on the spin of the hole, $\varepsilon\simeq 1.-10$ for $0.92\leqslant a\leqslant 0.98$ (cf. Fig. 4).

Next, let us relate the energy emitted by the sequential infall of N clumps of mass δM through r_+ to the amplitude of the waveform in the time domain. Assume N to be small enough such that $N\delta M < M_{\rm initial}$ but large enough to enable us to arrive at a sensible average of the rms strain amplitude over the corresponding number of wave

[5] Quasi-normal modes are strongly damped because of the boundary conditions of purely ingoing radiation at r_+ which saps most of the energy emitted by the metric perturbation unless the waves are strongly beamed from relativistic motion (Sterl Phiney, private communication). In this sense, the damping of the mode corresponds to radiation reaction with most of the energy being advected in by the hole.

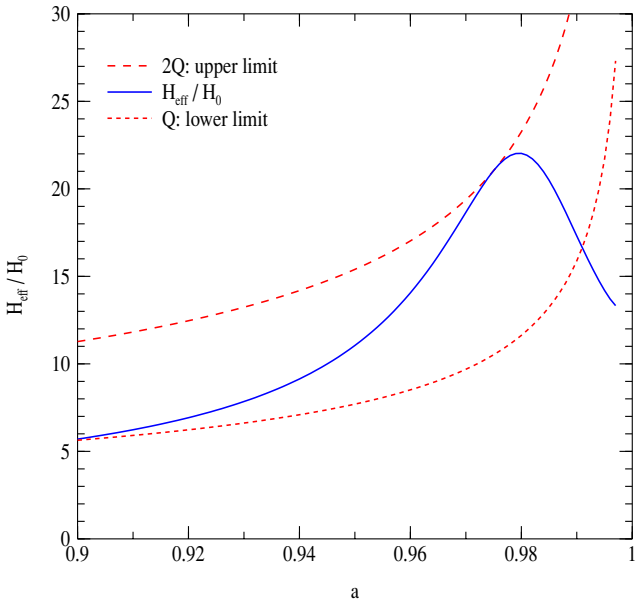

Figure 4. The solid line indicates the augmented amplitude of QNR oscillations driven near resonance by clumpy hyper-accretion from a neutrino-cooled disc as a function of the spin parameter, a, of the hole. Modulo a small spread caused by the stochasticity in time arrival of the clumps to $r_{\rm mb}$ (see discussion in the text), the enhanced amplitude lies within the curves for Q(a) and 2Q(a) throughout the range $a > 0.9$. A brisk energy deposition rate $\propto (H_{\rm sat}/H_0)^2$ ensues.

cycles. The energy flux averaged over N cycles is (Isaacson 1968)

$$\frac{{\rm d}E}{{\rm d}A\,{\rm d}t} = \left(\frac{c^3}{G}\right)\frac{1}{16\pi}\langle\dot{h}(t)\cdot\dot{h}^*(t)\rangle. \quad (14)$$

With $h(t)$ as given by equation (13) and assuming no spin evolution, $\dot{a}\doteq\emptyset$, the total energy radiated in gravitational waves results from integrating equation (14) over an encompassing surface (recall $\int{\rm d}\Omega|S_{22}|^2 = 1$), and over a time interval corresponding to N cycles of $\omega_{\rm dr}$:

$$E_{\rm GW} = \left(\frac{c^3}{8G}\right)N\omega_{\rm dr}\,|H_{\rm sat}|^2. \quad (15)$$

On the other hand, an approximate estimate of the total GW energy deposition which accounts for a slight mass increment of the black hole without spin evolution is as follows. First, write the energy emitted during one driven cycle as $\delta E = c^2(\varepsilon\,\delta M)\delta M/M_{\rm initial}$, and note that the clump mass is $\delta M\simeq\dot{M}\Omega_+^{-1}(r_{\rm mb})\propto M$ (constant a and $\dot{M}$). For $\Delta M\equiv\Sigma\delta M < M_{\rm initial}$, replace the factor in parentheses by the geometric mean of δM over the hyper-accreting epoch, $\delta\bar{M}$, and perform the integral of $\delta M/M(t)$ by writing $\delta M = \dot{M}\,{\rm d}t$. This yields

$$\Delta E_{\rm GW} = c^2\,\varepsilon\delta\bar{M}\,\ln\left(\frac{M_{\rm final}}{M_{\rm initial}}\right) \quad (16)$$

where ε may be larger than unity for black hole spins in excess of $a\gtrsim 0.92$.

5 DETECTABILITY CRITERION

Rather than attempt to describe the complex time evolution of the gravitational waveform throughout the hyper-accreting stage, we will simply assess the detectability of the waves with the matched

filtering technique by utilizing the above energy estimate, equation (16), while focusing on a relatively short time interval such that the mass added to the hole is a small fraction of the initial mass.

For definiteness, we adopt $M_{\rm initial} = 15\ {\rm M}_\odot$ ($f \simeq 2147$ Hz) and $\Delta M = 1\ {\rm M}_\odot$ corresponding to a second of hyper-accretion at $\dot{M} = 1\,{\rm M}_\odot\,{\rm s}^{-1}$. Under the simplified model for the probability distribution of the clump mass as outlined above (quasi-linear analysis), a large fraction of the mass in the locus $r_{\rm mb} \leqslant r \leqslant r_{\rm ms}$ at any given time resides in a clump by the time fluid particles reach $r_{\rm mb}$. We estimate the mass in this clump to be $\delta M = \dot{M}\Omega_+^{-1}(r_{\rm mb})$ which is a factor of 2π smaller than the total mass in the annulus for fully wrapping, in-spiral trajectories, Section 4.2.

We follow Flanagan & Hughes (1998) to evaluate the likelihood of detection of GW from driven QNR modes by the LIGO interferometers. The criterion for detectability of the wave train through the matched filtering technique is a non-trivial signal-to-noise (S/N) ratio

$$\langle [{\rm S/N}]^2 \rangle = \int {\rm d}\ln\omega\, \frac{h^2_{\rm char}(\omega)}{h^2_{\rm noise}(\omega)} \tag{17}$$

where $h_{\rm noise}(\omega)\,[= h_{\rm noise}(f)/\sqrt{2\pi}]$ reflects the detector spectral density of strain noise appropriately averaged for random incident orientations with respect to the LIGO interferometers. The characteristic strain amplitude of the wave train is given by

$$h^2_{\rm char}(\omega) \equiv \frac{2(1+z)^2}{\pi^2 d^2}\frac{{\rm d}E}{{\rm d}\omega}[(1+z)\omega], \tag{18}$$

where d is the luminosity distance to the source, z the redshift, and ω the observed angular frequency. Defined this way, $h_{\rm char}$ is not trivially related to the amplitude of the strain in the time domain, $H_{\rm sat}$, nor to the same in the frequency domain. Rather, it is a gauge of the time-integrated power spectrum weighted by the 'monochromaticity' of the wave train over the observation time.

With $(1+z)\omega \to \omega$, the GW energy spectrum from driven QNR modes in the radiation zone,

$$\frac{{\rm d}E(\omega)}{{\rm d}\omega} = \frac{\omega^2}{16\pi^2}\,\tilde{H}(\omega)\cdot\tilde{H}^*(\omega), \tag{19}$$

ensues from a Fourier transform of the strain signal in the time domain as given in equation (13) (compare this expression with equation 2.38 of Flanagan & Hughes 1998, and note the conforming notation used throughout).

Let us approximate all quantities $\propto M$ by their geometric mean and assume no spin evolution during a small epoch of hyper-accretion $T = 2\pi N/\omega_{\rm dr}$ (with $\log\ N$ in the range 3–3.5). With $\tilde{H}(\omega) = 2H_{\rm sat}{\rm e}^{{\rm i}\delta_t}\sin(N\pi\Delta\omega/\omega_{\rm dr})/\Delta\omega$ (note that $\dot{a} \doteq 0$ implies $\delta_t =$ constant as well), the characteristic strain amplitude of driven QNR waves turns out to be

$$h^2_{\rm char}(\omega) \equiv \frac{8(1+z)^2}{(2\pi)^4}\frac{H_{\rm sat}\cdot H^*_{\rm sat}}{d^2}\left[\frac{N\pi\omega}{\omega_{\rm dr}}\,\frac{\sin(x-b)}{x-b}\right]^2 \tag{20}$$

where $x - b \equiv N\pi(\omega-\omega_{\rm dr})/\omega_{\rm dr}$.

The strength of the characteristic strain signal at the driving frequency $\omega = 2\Omega_+(r_{\rm mb})$ follows by setting the expression in the square brackets to $[N\pi]^2$ and by utilizing equation (15) to replace $|H_{\rm sat}|^2$ in favour of the energy released during the hyper-accreting epoch $\Delta E_{\rm GW}$ as given by equation (16)

$$\begin{aligned} h^2_{\rm char}\big|_{\omega=\omega_{\rm dr}} &= \left(\frac{G}{c^3}\right)\left(\frac{2(1+z)}{\pi d}\right)^2\frac{N\Delta E_{\rm GW}}{\omega_{\rm dr}} \\ &= \left(\frac{G}{2\pi c}\right)\left(\frac{2(1+z)}{\pi d}\right)^2\varepsilon\delta\bar{M}\,T\,\ln\left(\frac{M_{\rm final}}{M_{\rm initial}}\right). \end{aligned} \tag{21}$$

For GRB 030329, we plug in $z = 0.1685$, $d = 810$ Mpc ($H_0 = 70$, $\Omega_{\rm b} = 0.3$, $\Omega_{\rm v} = 0.7$), $M_{\rm initial} = 15\ {\rm M}_\odot$, $T = 1$ s, and $\delta\bar{M} = \dot{M}\Omega_+^{-1}(r_{\rm mb}) \simeq 1.83_{-4}\,{\rm M}_\odot$ and choose $a = 0.98$ ($H_{\rm sat}/H_0 = 22$) to obtain $h_{\rm char} \simeq 8.4_{-23}$ at the observed linear frequency $f = 1490$ Hz. Utilizing similar parameters for GRB 980425 at $d = 27$ Mpc, produces a characteristic signal $h_{\rm char} \simeq 2.16_{-21}$ at $f \simeq 1741$ Hz.

6 DISCUSSION

We have laid out a physically motivated – if simple minded – model for resonant driving of the quasi-normal ringing (QNR) modes of the Kerr geometry. A nascent black hole hyper-accreting at rates $\dot{M} \approx 1\,{\rm M}_\odot\,{\rm s}^{-1}$ from a neutrino-cooled disc is reckoned to oscillate near resonance of its (l, m = 2, 2) quadrupole QNR frequency due to the infall of compact mass overdensities from the cusp in an effective potential on a dynamical time-scale. The model is based on large-scale, magnetorotationally induced fluid dynamics in the ultrarelativistic region of the flow bounded from below by the marginally bound orbit radius $r_{\rm mb}$ (assumed to coincide with the aforementioned cusp). Simulations that include black hole spin but no diffusive stress, i.e. De Villiers et al. (2003) and Hirose, Krolok & De Villiers (2004), seem to support the basic conclusion that the most unstable modes go to large scale as the photon orbit is approached (although this is cast in a different language, i.e. that the flow becomes more 'laminar' as the event horizon is approached). The relativistic linear mode analysis shows that this effect is very pronounced for relatively high values of the spin parameter: $a \geqslant 0.95$ (Araya-Góchez 2002). Unfortunately, the models KDP ($a = 0.90$) and KDE ($a = 0.998$) of De Villiers et al. (2003) seem inadequate to address this issue fully since in KDP the spin is not large enough and in KDE the Boyer–Lindquist coordinate distance between $r_{\rm ms}$ and $r_{\rm mb}$ is very small.

Long time-scale accretion rate fluctuations ($\delta t \gg \Omega_+^{-1}$) should have little impact on the proposed mechanism unless the accretion flow is completely starved/arrested on stochastic time intervals. Otherwise, long time-scale variations in the mean accretion rate simply translate into variable clump mass. Since excitation of the resonance is a collective effect, this is far less important than semiregular clump formation within the relativistic annulus. At shorter time-scales ($\delta t \simeq \Omega_+$), simulations that include black hole spin (e.g. De Villiers et al. 2003; Hirose et al. 2003) yield rms fluctuations in the mass accretion rate of order 20 per cent near $r_{\rm ms}$. Large-scale mode effects imply that some of the small overdensities will act as seed perturbations for the growth of heavier clumps by aggregation.

The exact location of the cusp in the effective potential will change the dynamical time-scale for infall but not by much when the spin parameter is $a \geqslant 0.9$. Furthermore, since the MRI time-scale is suitably fast, a small delay to reach the free-fall stage is all that is needed for MRI dynamics to act. Heat conduction from neutrino diffusion out of mass overdensities on the time-scale of the instability warrants that compressive perturbations on the linear MRI scale behave inelastically (Araya-Góchez & Vishniac 2004). This leads to sufficiently long-lived clumps in a highly intermittent medium. When the spin parameter of the hole exceeds 90 per cent, large-scale magnetorotational wave modes will segregate compact matter overdensities from large-scale magnetic field domains. The subsequent infall of these clumps from $r_{\rm mb}$ will drive the QNR modes of the geometry in resonant fashion if the clumps arrive at $r_{\rm mb}$ steadily, with a small spread around time intervals of $\mathcal{O}(\Omega_+^{-1})$, and for long enough to build the strain amplitude up to saturation.

Given the approximate nature of the quasi-linear arguments invoked to construct the model – i.e. taking the linear MRI as the driving force at the outer scale of the turbulence (see Winters et al. 2003) – it is difficult to address the probability distribution for clump arrival times from the linear theory alone. Nevertheless, we have argued that for large-mass clumps, $\delta M \simeq \dot{M}\Omega_{+}^{-1}$, the arrival times at $r_{\rm mb}$ will not be entirely stochastic since 'the bucket needs time to fill-up', nor entirely coherent since the seed density perturbations are stochastic but large-scale MRI dynamics will work to minimize the impact of this initial small-scale randomness. Thus, although accurate clump-mass/arrival-time distributions are outside the scope of this paper, the possibility of resonant driving of the modes is very sensible.

If the QNR modes are fed resonantly for a few seconds of hyper-accretion, the enhanced amplitude of the oscillations yields a very high rate of energy deposition into gravitational waves. Indeed, the integrated energy deposition is large enough to 'evaporate' the equivalent of a factor of a few times the total rest-mass energy of a single clump into gravitational waves. Unfortunately, the characteristic frequency of emission resides on a less than optimal range with respect to the advanced LIGO noise curve: $f \simeq 8000$–1600 Hz for $M \simeq 3$–$15\ {\rm M}_{\odot}$. On a more optimistic note, the high quality and degree of coherence of the expected signal should make this model a prime candidate for narrow-band LIGO searches. For gamma-ray bursts at low redshifts, this may ultimately lead to a signal strong enough to be seen by LIGO II.

A 15-$\rm M_{\odot}$ black hole accreting at 1 $\rm M_{\odot}\ s^{-1}$ may come about from the death throes of a very massive star. If such an explosion is associated with a long GRB, and the broad properties of the prompt gamma-ray light curve, to inner engine activity, hyper-accretion on to this heavyweight, fast spinning hole should be associated with a second broad hump in the gamma-ray light curve. We anticipate that gravitational waves with the predicted properties may be present at this stage of the GRB. The proposed mechanism is thus a direct probe of the elusive inner engine of gamma-ray bursts.

ACKNOWLEDGMENTS

It is a great pleasure to acknowledge stimulating and instructive discussions with Sterl Phinney, Lee Lindblom, Kip Thorne, Ethan Vishniac and Roger Blandford. I am greatly indebted to the Theoretical Astrophysics and Relativity Group at Caltech for their hospitality and to Don Juan's teachings: '. . . because the warrior, having chosen a path, has but one goal: to traverse its full length'.

REFERENCES

Abramowicz M., Jaroszynski M., Sikora M., 1978, A&A, 63, 221
Agol E., Krolik J., 1998, ApJ, 507, 304
Araya-Góchez R. A., 2002, MNRAS, 337, 795
Araya-Góchez R. A., Vishniac E. T., 2004, MNRAS, in press (doi:10.1111/1365-2966.2004.08329.x) (this issue)
Balbus S. A., 2001, ApJ, 562, 909
Blaes O., Socrates A., 2001, ApJ, 553, 987
Blandford R., Begelman M., 1999, MNRAS, 303, L1
Blandford R., Begelman M., 2004, MNRAS, 349, 68
Curry C., Pudritz R., 1995, ApJ, 453, 697
Davis M., Ruffini R., Press W., Price R., 1971, Phys. Rev. Lett., 27, 1466
De Villiers J. P., Hawley J. F., Krolik J. H., 2003, ApJ, 599, 1238
Di Matteo T., Perna R., Narayan R., 2002, ApJ, 579, 706
Echeverria F., 1989, Phys. Rev. D, 40, 3194
Flanagan E., Hughes S., 1998, Phys. Rev. D, 57, 4535
Foglizzo T., 1995, PhD thesis, Univ. Paris VII
Foglizzo T., Tagger M., 1995, A&A, 301, 293
Fryer C., Holz D., Hughes S., 2002, ApJ, 565, 430
Gammie C. F., Popham R., 1998, ApJ, 498, 313
Hawley J. F., Balbus J. H., 2002, ApJ, 573, 738
Hawley J. F., Krolik J. H., 2001, ApJ, 548, 348
Hirose S., Krolok J. H., De Villiers J.-P., Hawley J. F., 2004, ApJ, 606, 1083
Isaacson R. A., 1968, Phys. Rev., 166, 1272
Kozlowski M., Jaroszyński M., Abramowicz M., 1978 A&A, 63, 209
Krolik J. H., 1999, in Ostriker J. P., David N., eds, Active Galactic Nuclei: From the Central Black Hole to the Galactic Environment, Princeton Series in Astrophysics. Spergel Princeton Univ. Press, Princeton
Leaver E. W., 1985, Proc. R. Soc. Lond. A, 402, 285
Lousto, Price, 1997, Phys. Rev. D, 55, 2124
MacFadyen A. I., Woosley S. E., Heger A., 2001, ApJ, 550, 410
Narayan R., Yi I., 1995a, ApJ, 444, 231
Narayan R., Yi I., 1995b, ApJ, 452, 710
Narayan R., Igumenshchev I., Abramowicz M., 2000, ApJ, 539, 798
Novikov I., Thorne K., 1973, in DeWitt C., DeWitt B. S., eds, Black Holes. Gordon & Breach, New York, p. 343
Ogilvie G. I., Pringle J. E., 1996, MNRAS, 279, 152
Popham R., Gammie C. F., 1998, ApJ, 504, 419
Popham R., Woosley S., Fryer C., 1999, ApJ, 518, 356
Rybicky G., Lightman A., 1979, Radiative Processes in Astrophysics. John Wiley, New York
Shakura N. I., Sunyaev R. A., 1973, A&A, 24, 337
Teukolsky S., 1973, ApJ, 185, 635
Thorne K. S., 1987, in Hawking S., Israel R., eds, 300 Years of Gravitation. Cambridge Univ. Press, Cambridge
Turner N., Stone J., Sano T., 2002, ApJ, 566, 148
Turner N. J., Stone J. M., Krolik J. H., Sano T., 2003, ApJ, 593, 992
Winters W. F., Balbus S. A., Hawley J. F., 2003, MNRAS, 340, 519
Zerilli F. J., 1970, Phys. Rev. D, 2, 2141

This paper has been typeset from a TEX/LATEX file prepared by the author.